

Supplemental methods

Reagents and cell lines

Standard, molecular-biology-grade chemicals and buffers were purchased from Sigma, Thermo Fisher and VWR. CDK4/6 inhibitor (palbociclib), CXCR4 antagonists (motixafortide, HY-P0171 and plerixafor, HY-10046) and c-Myc inhibitor (10058-F4) were purchased from MedChemExpress (MCE). Importin inhibitor (importazole, 401105), and exportin inhibitor (leptomycin B, L2913) were purchased from Sigma. Protein kinase was purchased from ProQinase. Nuclear extraction kits were purchased from Active Motif (40410). KOPK1, JURKAT, DND41, MOLT4 and MOLT16 cells were a generously gift from Dr. Peter Sicinski's lab, Harvard Medical School. Cells were cultured in RPMI-1640 supplemented with 10% FBS. Melanoma cell lines (WM9, MNT-1, SK-MEL-28, 501Mel) were from Dr. Kenneth D. Tew's lab, MUSC. Melanoma cells were cultured in RPMI-1640 supplemented with 10% FBS except that MNT-1 cells were cultured in 70% DMEM, 20% FBS, 10% AIM-V medium supplemented with 1X non-essential amino acids.

Antibodies

Antibodies against the following proteins were used for immunoblotting and/or immunofluorescent staining: CDK6 (Cell signaling, 3136, RRID:AB_2229289); CXCR4 (Sigma, SAB3500383, RRID:AB_10637698 or Invitrogen, 35-8800); cyclin D3 (Abcam, ab28283); lamin A/C (Santa Cruz, SC-376248, RRID:AB_10991536); tubulin (Sigma, T9026); actin (Proteintech, 66009-1-Ig); PFKP (Cell Signaling, 5412, RRID:AB_10694260 for western blotting; Proteintech, 13389-1-AP for IHC, RRID:AB_2252278; Santa Cruz, sc-514824 for immunoprecipitation); GST (Cell Signaling, 2622); HIS (Santa Cruz, SC-803); FLAG (Sigma, F1804); Anti-Flag M2 affinity gel (Sigma, A2220); GAPDH (Cell Signaling, 5174); CRM1 (Cell signaling, 13684T and 46249S); GFP (Cell Signaling, 2956 for western blotting; Invitrogen, A11120 for immunoprecipitation); importin-9 (Proteintech, 177551-AP; Invitrogen, 01-675-524); HMMR (Proteintech, 15820-I-AP); VEGFA (Proteintech, 66828-I-Ig); FGFR3 (Proteintech, 66954-I-Ig); RB1 (Santa Cruz, SC-50); RBL1 (Santa Cruz, SC-318); RBL2 (Santa Cruz, SC-317); c-Myc (Cell signaling, 5605S for western blotting; Invitrogen, MA1-980 for CHIP); phosphor-c-Myc (S62) (Abcam, ab51156); pT58-c-Myc (Abcam, ab185655); human CD45 (Cell Signaling, 13917 for IHC; Biolegend, 304032 for FACS).

Plasmids

DNA sequences encoding PFKP were cloned into Bam HI and SnaBI sites of pBABE-hygro retroviral vector as previously described by us (1). Oligonucleotide primers encoding putative

NESs or NLSs were cloned into BamHI of pMXs-GFP/puro retroviral vector (AddGene). The oligonucleotide primers used to construct GFP-NES/NLS are listed in **Supplemental Table 3**. The shRNA constructs against PFKP, CDK6, cyclin D3, RB1, RBL1 and RBL2 have been described previously (1). The shRNA constructs against importin-9 (TRCN0000336887), c-Myc (TRCN0000174055, TRCN0000039642) and CXCR4 (TRCN0000256866, TRCN0000256864) were purchased from Sigma-Aldrich MISSION. shRNA constructs against p53 (25636 and 25637) were from Addgene. Mutations of RXL motifs in PFKP were made using the Quikchange II XL site-directed mutagenesis kit (Agilent Technologies) with the primers for RXL mutations shown in **Supplemental Table 3**. An SV40 NLS (MDPKKKRKGR) signal sequence was added at the N-terminal of PFKP in pBABE-hygro retroviral vector with the primers shown in **Supplemental Table 3**.

RT-PCR

For qRT-PCR, total RNA extracted with RNA RNeasy mini kit (Qiagen) was reverse-transcribed to cDNA using reverse transcriptase (Bio-Rad), and qRT-PCR was performed in BioRad CFX96 Touch Real-Time PCR detection system with specific primers.

Luciferase reporter assay

For luciferase reporter assay, GLuc-ON™ dual-reporter clones containing human CXCR4 promoter were purchased from GeneCopoeia. The CXCR4 promoter clones were transfected into DND41 leukemia cells (stably expressing WT-, NLS-, S679E-PFKP individually) using lentiviral transduction, and the transfected cells were selected by puromycin. Cell culturing media was collected and Secrete-Pair dual luminescence assay (GeneCopoeia) was applied to detect the activity of the promoter by following the manufacturer's instructions. The promoter activity was reported using the signal ratio of Gluc to SEAP (internal control) to eliminate the impact of transfection efficiency variation. Luminescence was recorded using a VICTOR3 multilabel plate reader (PerkinElmer). Three biological replicates were measured.

Chromatin Immunoprecipitation (ChIP)

ChIP was performed according to published protocols with slight modifications (2-4). Formaldehyde was added to cell culture media to a final concentration of 1%. After 10 min fixation was stopped by the addition of 2.5M glycine to a final concentration of 0.125M (1/20 volume) at room temperature. Fixed cells were collected by centrifugation and washed with cold PBS. Then fixed cells were swelled in cell lysis buffer (5 mM Pipes pH 8.0, 85 mM KCl, 0.5% NP40)

supplemented with protease inhibitors on ice for 20 min. The nuclear pellet was collected by centrifugation at 6,000 rpm for 5 min, washed with cold PBS, and resuspended in nuclei lysis buffer (1% SDS, 10 mM EDTA, 50 mM Tris-HCl pH 8.0) supplemented with protease inhibitors on ice for 10 min. The chromatin was sheared by sonication on ice to an average size of 500 bp. Samples were centrifuged at 12,000 rpm for 10 min at 4°C, and supernatant was collected into an Eppendorf tube. Samples were diluted 10-fold in IP dilution buffer (0.01% SDS, 1.1% Triton X-100, 1.2 mM EDTA, 167mM NaCl, 16.7mM Tris-HCl pH 8.0) supplemented with protease inhibitors. Protein A/G plus agarose beads were blocked with 1 µg/µl salmon sperm DNA (Invitrogen 15632-011) and 1 µg/µl BSA for 4 hr at 4°C. Then protein A/G plus agarose beads were incubated with supernatants on a rotation wheel for 15 min at 4°C to preclear the chromatin solution. Samples were spun down at 2,000 rpm at 4°C, and supernatant was collected in a fresh tube. Precleared chromatin from 2.5×10^7 cells was incubated with 1 µg of primary antibody, mouse IgG or no antibody at 4°C overnight. The next day, 40 µl protein A/G plus agarose beads were added, and incubated on a rotating wheel for 2 hr at 4°C. Samples were collected by centrifugation at 2,000 rpm at 4°C. The supernatant from the reaction with no primary antibody was kept as total input chromatin. Immunoprecipitates were washed twice with 1 ml low salt buffer (0.1% SDS, 0.1% Triton X-100, 2 mM EDTA, 150mM NaCl, 20mM Tris-HCl pH 8.0), twice with 1 ml high salt buffer (0.1% SDS, 0.1% Triton X-100, 2 mM EDTA, 500mM NaCl, 20mM Tris-HCl pH 8.0), twice with 1 ml IP wash buffer (0.5 M LiCl, 1% NP-40, 1% deoxycholic acid, 100mM Tris-HCl pH 9.0) and twice with 1 ml TE buffer. Immunoprecipitated DNA was eluted with fresh elution buffer (1% SDS, 0.1M NaHCO₃ pH8.0) by vortexing for 10 min. Formaldehyde crosslinks were reversed by adding 5M NaCl to a final concentration of 0.3M. 10 µg of RNase A was added to remove RNA, followed by incubation at 65°C for 6 hr. Two volumes of ethanol were added to precipitate DNA/proteins at -20°C overnight and pelleted by centrifugation. Samples were resuspended in 100 µl of TE buffer, 25 µl of 5 x proteinase K buffer (1.25% SDS, 25 mM EDTA, 50mM Tris-HCl pH 7.5), 1.5 µl of proteinase K and incubated at 42°C for 2 hr. Qiaquick PCR purification kits (Qiagen) were applied to extract DNA samples.

Cell cycle analysis

The BrdU-PI staining method was applied to determine cell cycle phases. Cells were incubated in culture media containing 75 µM 5-bromo-2'-deoxyuridine (BrdU) for 1 hr, then harvested via centrifuge and fixed in 90% ethanol overnight. Fixed cells were spun down and washed with PBS. Then cells were treated with 2N HCl containing 0.5% Triton X-100 for 30 min at room temperature before resuspending in borate buffer at pH 8.5. Then cells were incubated with an anti-BrdU

antibody (556028, BD Biosciences) for 30 min. After spinning down, cells were incubated with 5 µg/ml propidium iodide and 200 µg/ml RNase A for 30 min and washed with staining buffer, then analyzed by flow cytometry (BD LSR Fortessa).

Cell apoptosis assay

Cell apoptosis was quantified using the Annexin V apoptosis detection kit (eBioscience, 88-8006-72). In brief, 2×10^6 KOPTK1 cells expressing either WT-PFKP, NLS-PFKP or PFKP-RXL were collected and suspended in binding buffer (eBioscienc). Cells were stained with fluorochrome-conjugated Annexin V, and with propidium iodide, then analyzed by flow cytometry (BD LSR Fortessa).

Immunoprecipitation (IP) and immunoblotting

In brief, 20 µl (10 µg) PFKP AC conjugated IgG beads (Santa Cruz, SC-514824AC) were incubated overnight with 1-3 mg of whole cell lysate in IP lysate buffer (Pierce) at 4 °C. An equal amount of mouse IgG was applied as a control. The precipitated protein complex was washed with Phosphate Buffered Saline Tween-20 (PBST) three times and denatured with 2XSDS-PAGE buffer at 95 °C for 8 min. The immunoprecipitated protein complex was separated in 10% SDS-PAGE gel and transferred to nitrocellulose membranes (0.45 µM). The membrane was blocked with 5% BSA in TBS for 30 min and incubated overnight with primary antibody at 4 °C. The signal was detected with a chemiluminescence imaging system with CCD camera (BioRad Molecular Imager or LI-COR Biosciences Odyssey). Anti-Flag M2 affinity gel (Sigma, A2220) was used to IP exogenous FLAG-PFKP-WT or FLAG-PFKP-RXL mutant. Anti-GFP (Invitrogen) was used to IP GFP-NLS or GFP-NES fusion proteins. Immunoblots were quantified with ImageJ.

Flow cytometry to determine the expression of CXCR4

1×10^6 leukemia cells were collected and washed three times with PBS, then fixed with 4% formaldehyde for 20 minutes. For cellular surface CXCR4 staining, fixed cells were pre-blocked in blocking buffer (PBS with 2% BSA) for 1 hr, then stained with anti-CXCR4 antibodies (1:100, Sigma, in PBS with 2% FBS) or control IgG for 30 min on ice followed with FITC conjugated anti-rabbit secondary antibodies (1:10,000). The stained cells were then washed and analyzed by flow cytometry. For intracellular CXCR4 staining, fixed cells were treated with 0.5% Triton for 10 minutes followed with blocking and antibody incubation.

Viral transduction and transfection

Retroviral and lentiviral plasmids were packaged in HEK293T cells seeded in 10-cm petri dishes one day before transfection. Lipofectamine 2000 was applied for transfection. The expression plasmids were co-transfected with the packaging plasmid (pCMV-Gag-Pol for retroviral infections; pCMV-delta8.9 for lentiviral infections) and the envelope plasmid (pCMV-VSV-G). Plasmid ratios of pCMV-VSV-G/pCMV-Gag-Pol/expression plasmid 3:5:10 for retroviral transductions, and the ratio of pCMV-VSV-G/pCMV-delta8.9 /expression plasmid 1:5:10 for lentiviral transductions were used. Virus-containing medium was harvested two days after transfection, filtered and concentrated with high-speed ultracentrifugation at 21,000 RMP for 1.5 hr. The virus pellet was resuspended in fresh media on ice for 30 min. For suspension infection, 1×10^6 leukemia cells were seeded in a 6-well plate with retrovirus in the presence of 10 μ g/ml polybrene. The plate was spun for 1.5 hr at 1,800 rpm at 32 °C. The infected cells were incubated for 6 hr and refreshed with media. Two days after infection, selection reagent was added with fresh cell culture media.

Seahorse extracellular flux analysis of glycolysis and mitochondrial respiration

ECAR (glycolysis) and OCR (mitochondria respiration) were measured using a Seahorse XF24 analyzer (Agilent Technologies). Seahorse culture plates were coated with Corning® Cell-Tak™, Cell and Tissue Adhesive (#354240) 24 hr before leukemia cells were seeded. DND41 cells were cultured in mixed medium (RPMI-1640+DMEM medium (1:1) supplemented with 5% FBS) for 12 hr before analyses. 1×10^5 DND41 cells/150 μ l per well were washed and seeded in the XF24 microplate with conditional medium (culture medium without FBS and sodium bicarbonate). The final concentrations of glucose, oligomycin and 2-deoxy-D-glucose (2-DG) were 10mM, 1 μ M, and 50mM, respectively.

Immunohistochemistry staining of formalin-fixed paraffin-embedded human lymph node specimens from patients with T-cell lymphoma/leukemia

Tissue samples of T-cell lymphoma, control lymph node and thymus were obtained with informed consent from Tongji Hospital of HUST. The specimens were isolated at the time of biopsy or surgery, formalin fixed and paraffin embedded, and stained with H&E. The diagnosis of different types of T-cell lymphoma or control lymph was confirmed based on histological findings by two independent pathologists according to the 2016 World Organization classification. Standard immunohistochemistry (IHC) was performed with individual antibody against PFKP (13389-1-AP, Proteintech), CXCR4 (11073-2-AP, Proteintech) or CDK6 (PB1047, Boster). For PFKP status, nuclear PFKP staining observed in more than 5% of total cells in the samples was assigned as a

positive score. Ten random fields in each slide were assessed by the pathologists in a blinded fashion.

IHC was performed on 3 µm formalin-fixed paraffin-embedded (FFPE) tissue sections baked for 1 hour at 60°C. Following the manufacturer's instructions, all sections were deparaffinized with xylene and rehydrated through a series of descending graded alcohols. Antigen retrieval was performed in citrate buffer (pH 6.0) in a pressure cooker for 1.5 minutes at 120°C. Endogenous peroxidase activity was blocked by using 3% H₂O₂ for 10 min. Sections were then incubated with primary antibodies: PFKP (13389-1-AP, Proteintech); CXCR4 (11073-2-AP, Proteintech); CDK6 (PB1047, Boster) overnight at 4°C, followed by a peroxidase-conjugated polymer (Dako REAL EnVision/HRP, Rabbit/Mouse (ENV) reagent of the kit k5007, Denmark) for 30 min at 37°C. To reveal the immune staining, the sections were incubated with Dako REAL DAB+ Chromogen for 5 min (Dako k5007, Denmark), followed by counterstaining with hematoxylin, then dehydration and mounting. PBS instead of primary antibody was used as a negative control.

Bioinformatic analysis

The RNA-seq expression values (RPKM) of 1,019 cell lines, including 176 hematopoietic cancer cell lines, were downloaded from the CCLE database (<https://portals.broadinstitute.org/ccle>) (5). Pearson correlation coefficients of each pair of genes were calculated using R v3.6.2 software. The PFKP interacting protein data were downloaded from the BioGRID database v3.5.185 (<https://thebiogrid.org/>) (6).

Gene Ontology analyses of the PFKP interacting protein: Gene Ontology (GO) analyses for enriched 'biological process' terms were performed using the web tool DAVID Bioinformatics Database v6.8 (<https://david.ncifcrf.gov/tools.jsp>) (7) for the 'GOTERM_BP_DIRECT' category. The complete set of all RefSeq genes was used as a background.

Cistrome data browser toolkit (<http://cistrome.org/db/#/>) was used to examine the potential transcription factors regulating CXCR4 expression and c-Myc DNA binding peaks on CXCR4 promoter region.

The c-Myc ChIP-seq and corresponding input control data of H2171 and HCT116 cell lines were downloaded from GEO database with the accession numbers: GSM894102, GSM894105, GSM894106 (H2171), and GSM2065882, GSM2065897 (HCT116). ChIP-seq reads were aligned to the non-random chromosomes of the human (hg38 assembly) genome using Bowtie2 v2.2.9 with default parameters (8). Peak calling was performed using MACS2 v2.1.1 (9) with

corresponding input controls (default parameter, except: q value cutoff = 0.01). BigWig file generation for each dataset was performed using deepTools v2.5.3 (10).

Supplemental figure legends

Figure S1. Related to Figure 1.

S1A & S1B. Quantification of PFKP expression for **1B (S1A)** and **1C (S1B)**. PFKP expression was normalized to nuclear PFKP from DND41 or KOPTK1 cells treated with DMSO control.

S1C & S1D. Immunoblotting of NESs (**S1C**) or NLSs (**S1D**) fused GFP protein in either nuclear extract (NE) or cytoplasmic extract (CE) from DU145 cells stably expressing NES- or NLS-GFP.

S1E. Nuclear enrichment of NES mutant of PFKP. Immunoblotting of ectopic PFKP using FLAG antibody in NE and CE from KOPTK1 cells.

A-D, n=3; E, n=2. Data represent mean \pm SEM. Two-tailed Student's t-test (A and B); *p < 0.05, **p < 0.01.

Figure S2. Related to Figure 2.

S2A. Left: Schematic depicts separation of dimeric PFKP from tetrameric PFKP by ultrafiltration (USY-20, Advantec MFS) with molecular weight (MW) cutoff of 200 kDa in cytoplasmic (CE) or nuclear extract (NE) of cells. Dimeric PFKP (MW 171 kDa) passes the filter, and tetrameric PFKP (MW 342 kDa) is retained. **Middle (DND41) & Right (KOPTK1):** Escalating amounts (10, 30 and 90 μ L) of filtrate (<200kDa) was resolved on SDS-PAGE along with 10 μ L of unfiltered nuclear or cytoplasmic extract. BRCA1 protein (208 kDa) was used to validate ultrafiltration. Immunoblotting (IB) for lamin A/C and tubulin demonstrates separation of cytoplasmic and nuclear fractions.

S2B. IB of NE showed PFKP expression was reduced in DND41 cells in which either cyclin D3 or CDK6 was knocked down. WCL = whole cell lysate.

S2C. Pull-down assay was applied to examine the interaction between purified FLAG-PFKP immunoprecipitated from lysate of KOPTK1 cells expressing FLAG-PFKP and recombinant cyclin D3/CDK6. Presence of cyclin D3/CDK6 in pull-down complex was identified by IB using antibody to His (CDK6) or GST (cyclin D3).

S2D. IB of FLAG tag shows no nuclear accumulation of PFKP-RXL mutant in cells treated with the exportin inhibitor leptomycin B (LMB) (5 ng/ml, 24 hr).

S2E. Immunoprecipitation (IP) followed by mass-spectrometry (MS) data shows CDK6 and PFKP interact with importin-9 in leukemia cells. **Left**, CDK6 interacts with importin-9 (data derived from Supplementary Table 1 of (1)). **Right**, PFKP interacts with importin-9. Anti-PFKP antibody conjugated agarose beads were applied for examination of PFKP interacting proteins (unpublished data, n=2). IgG conjugated agarose beads were used as controls.

S2F. IP using CDK6 antibody conjugated beads followed by IB shows importin-9 interacted with CDK6 in lysates of leukemia cells. IgG conjugated beads was a control.

S2G & S2H. IP with PFKP antibody followed by IB to test the disrupted interaction between PFKP and importin-9 in cells in which CDK6 was either inhibited with palbociclib (1 μ M, 24 hr) (**S2G**) or depleted with shRNA (shCDK6) (**S2H**).

S2I. IP with GFP antibody followed by IB identifies the interaction of importin-9 with a functional NLS (NLS3), and of CRM1 with functional NES (NES1 and NES2). The presence of importin-9 or CRM1 was identified with individual antibody. Ponceau S was applied to stain the heavy chain of GFP antibody (PS: HC).

A, n=4; B-D, F-I, n=3.

Figure S3. Related to Figure 3.

S3A. Representative immunoblotting of nuclear extract (NE) and cytosolic extract (CE) from KOPTK1 cells expressing WT-PFKP, NLS-PFKP or PFKP-RXL.

S3B. The glycolysis, glycolytic capacity and glycolytic reserve of DND41 cells expressing vector, WT-, NLS- or S679E-PFKP were assessed through extracellular acidification rate (ECAR) using Seahorse analyzer (Agilent).

S3C. Percentages of cell populations at different phases of cell cycle analyzed with BrdU/PI staining.

S3D. Relative cell numbers after 8 hr treatment as indicated. Cell numbers were normalized to cells without CXCL12 treatment.

A, C, n=3; B, n>=7; D, n=4. C&D represent mean \pm SEM; B is shown as mean \pm SD. Two-tailed Student's t-test (D); n.s., not significant.

Figure S4. Related to Figure 4.

S4A. CXCR4 expression measured by flow cytometry from cells in which RB, RBL1 and RBL2 were knocked down. The knockdown efficiency of RB, RBL1 and RBL2 were examined in whole cell lysate with immunoblotting. shRB represents the combinational knockdown of RB, RBL1 and RBL2.

S4B. Downregulation of CXCR4 expression by CDK6 inhibition does not involve p53. **Left:** The effect of palbociclib treatment on CXCR4 expression was measured by flow cytometry in p53 knocked down cells. p53 was knocked down with shRNA (shp53-1 or shp53-2). **Right:** Immunoblotting of whole cell lysate was applied to measure p53 knockdown efficacy.

S4C & S4D. CXCR4 expression measured by flow cytometry is upregulated in MOLT4 (**S4C**) and KOPTK1 (**S4D**) cells expressing NLS-PFKP.

S4E. PFKP knockdown with shRNA (shPFKP) reduces CXCR4 expression measured by flow cytometry in cells (**upper**). IB shows the knockdown efficiency of PFKP (**lower**).

S4F. CXCR4 mRNA levels are increased in MOLT4 cells expressing NLS-PFKP.

S4G. Grouped proteins interacting with PFKP according to analysis of the BioGRID database. Note that PFKP interacts with multiple transcription factors including c-Myc.

A-F, n=3. Data represent mean \pm SEM. Two-tailed Student's t-test (A-B and E) and 1-way ANOVA (C-D and F); *p < 0.05, **p < 0.01, ***p < 0.001.

Figure S5. Related to Figure 5.

S5A. Cistrome data browser toolkit (<http://cistrome.org/db/#/>) was applied to public ChIP-seq, DNase-seq and ATAC-seq data to discover transcription factors that regulate CXCR4. In the figure, regulatory potential (RP) is a score reflecting the likelihood that a factor regulates a gene. X axis is the RP score; Y axis represents different factors; factors are ordered using the maximum RP score. Each bold dot represents a ChIP-seq/DNase-seq/ATAC-seq sample. Horizontal row of dots at a given Y-axis value denotes the same factor. Regulatory potential of four transcription factors (c-Myc, ZBTB7A, SOX2, MECOM) binding to PFKP are shown.

S5B. c-Myc binding sites on the promoter region of CXCR4 (1,000 bp upstream of the transcription start site). Map was derived from ChIP-seq data from two cell lines (H2171 and HCT116) in which c-Myc has the highest regulatory potential at the CXCR4 promoter region according to the Cistrome Data Browser Toolkit analysis. Primers were designed for the indicated amplicon in ChIP assay.

S5C. Total cell numbers quantified for DND41 cells expressing ectopic PFKP, in which c-Myc was knocked down. 3×10^5 cells were seeded on Day 0, and total cell numbers were counted on Day 1.

S5D. JQ1 treatment decreases invasion capability of DND41 cells expressing ectopic PFKP. Invaded (**left**) and total (**right**) cell numbers were counted with/without JQ1 (0.5 μ M) treatment.

S5E. Total cell numbers quantified for DND41 cells expressing either WT-, NLS-, or S679E-PFKP upon treatment with the c-Myc inhibitor, 10058-F4 (50 μ M).

C & D (**left**), n=3; D (**right**) & E n=4. Data represent mean \pm SEM. 1-way ANOVA (D); ****p < 0.0001.

Figure S6. Related to Figure 6.

S6A. Left: Treatment with CXCR4 antagonist (motixafortide or plerixafor) dramatically decreases invasiveness of DND41 cells expressing ectopic PFKP. **Right:** Total numbers of CXCR4 antagonist-treated DND41 cells quantified before and after treatment.

S6B. Total cell numbers quantified for cell invasion assays of Figure 6A before and after treatment with CXCR4 antagonists.

S6C. Total cell numbers quantified for cell invasion assays of Figure 6B after CXCR4 knockdown.

S6D. IHC staining using human CD45 antibody of liver or bone marrow from mice that received KOPTK1 cells expressing either WT-, NLS-PFKP, or PFKP-RXL. Mice were treated with plerixafor (**lower**) or vehicle control (**upper**) for three weeks. Arrows indicate blood vessels. Scale bar is 100 μ M.

S6E. Cell proliferation determined as the percentage of Ki67⁺ cells over total human CD45⁺ cells using flow cytometry analysis in tissues (bone marrow, spleen or liver) from mice implanted with KOPTK1 cells expressing either WT-, NLS-PFKP, or PFKP-RXL. n=4 mice/group were measured.

S6F. Glycolysis inhibition prevents PFKP nuclear translocation. Representative immunoblotting of PFKP in nuclear extracts (NE) and cytosolic extracts (CE) of Jurkat and KOPTK1 cells treated with the glycolysis inhibitor 2-DG (50 mM, 24 hr).

S6G. Inhibition of glycolysis (50 mM 2-DG, 24 hr) downregulates CXCR4 expression as measured by flow cytometry in KOPTK1 (**left**) and MOLT4 (**right**) cells.

A(**left**), B-C, G, n=4; A(**right**), F, n=3; D, n=5 mice/group; E, n=4 mice/group. Data are mean \pm SEM. Two-tailed Student's t-test (G) and 1-way ANOVA (A and E); ****p < 0.0001 and n.s., not significant.

Figure S7. Related to Figure 7.

S7A and S7E. Relative primary T-ALL cell numbers of DFAT-24836 (**S7A**) or CBAT-93917 (**S7E**) following treatment with either CDK4/6 inhibitor (palbociclib, 1 μ M), CXCR4 antagonist (plerixafor, 10 μ M) or c-Myc inhibitor (10058-F4, 50 μ M) in the presence of CXCL12 (100 ng/ml) for 24 hr.

S7B. Nuclear PFKP expression in primary T-ALL cells CBAT-93917 following treatment with either palbociclib (palbo, 1 μ M), BSJ-03-123 (CDK6D, 10 μ M), or importazole (Impor, 40 μ M) for 24 hr.

S7C. CXCR4 expression analyzed with flow cytometry in primary T-ALL cells CBAT-93917 following treatment with either palbociclib (palbo, 1 μ M), BSJ-03-123 (CDK6D, 10 μ M), importazole (Impor, 40 μ M), or c-Myc inhibitor (10058-F4, 50 μ M) for 24 hr.

S7D. Cell invasion capability of primary T-ALL cells CBAT-93917 treated with either palbociclib (palbo, 1 μ M), plerixafor (10 μ M) or c-Myc inhibitor (10058-F4, 50 μ M) for 24 hr.

S7F. Immunoblotting of CDK6, cyclin D3, or PFKP expression in multiple melanoma cells lines.

S7G. CXCR4 expression measured with flow cytometry in multiple melanoma cell lines treated with CDK4/6 inhibitor (palbociclib, 1 μ M) for 24 hr.

A, D & E, n=4; B, C, F & G, n=3. Data represent mean \pm SEM. Two-tailed Student's t-test (G) and 1-way ANOVA (C and D). **p < 0.01, ****p < 0.0001 and n.s., not significant.

Figure S8. Related to Figure 8.

S8A. IHC staining of PFKP was performed on slides from normal (n=5) or hyperplastic (n=5) thymus.

S8B. Multivariate prognostic analysis of independent risk factors for overall survival (OS) in patients with AITL. Patients were grouped into stage I/II and stage III/IV for analyses in S8B and Table 4.

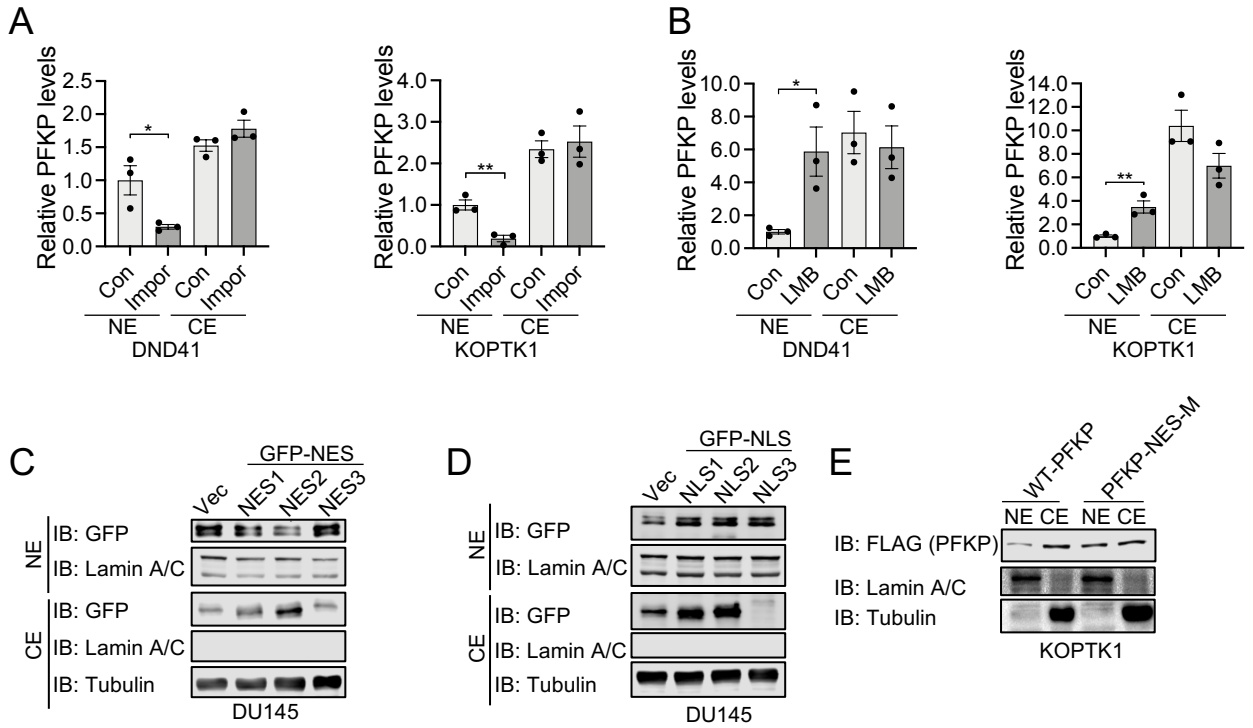
The Ann Arbor staging classification was applied. Age <60 and \geq 60 were applied for both analyses.

S8C. CDK6 expression positively correlates with that of CXCR4 in specimens from NK/T patients (n=14). IHC staining of CXCR4 or CDK6 was performed on a series of slides from the same tissue block. Normal (n=36) and Reactive Hyperplastic (n=16) lymph nodes were applied as controls.

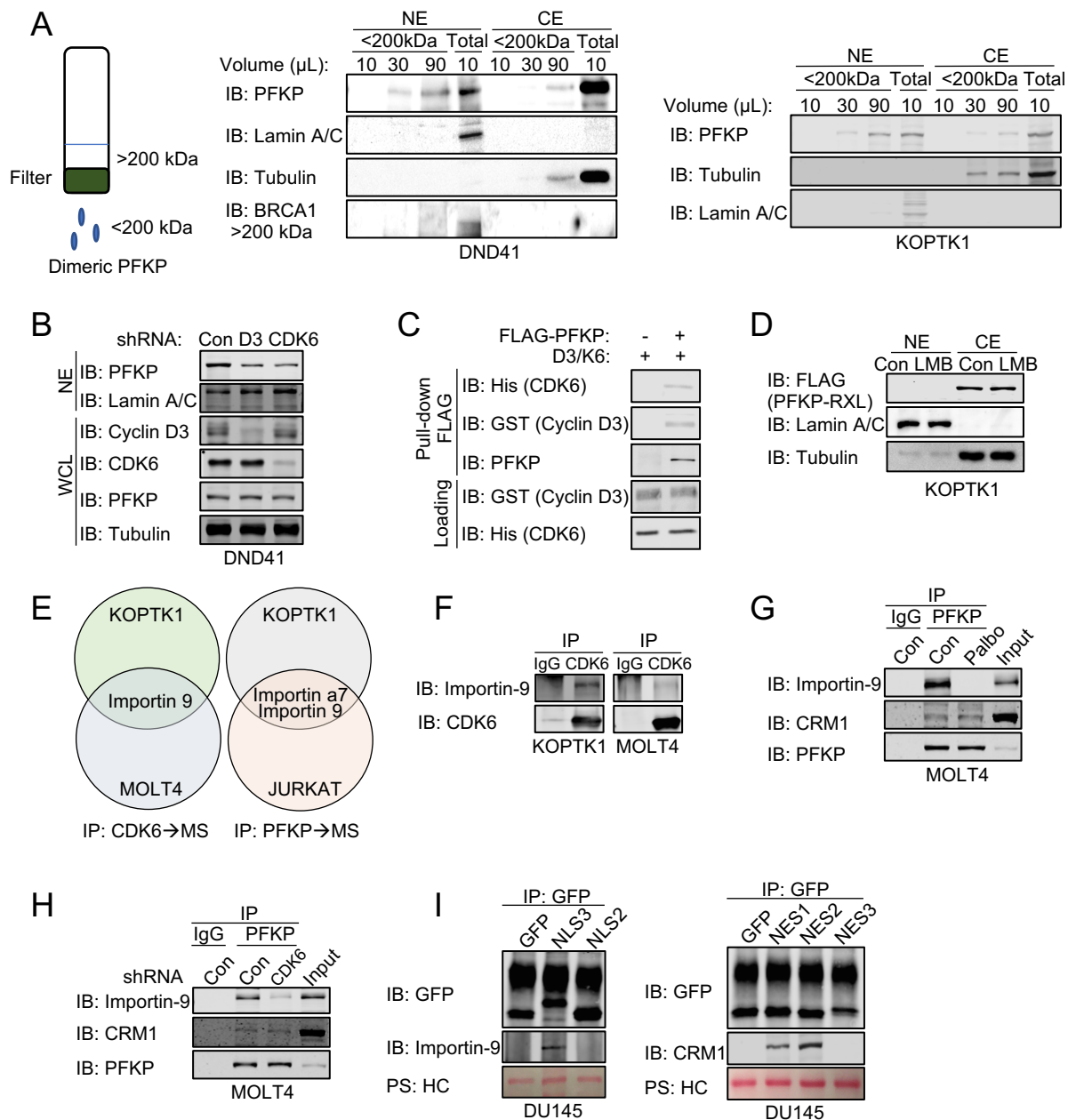
S8D. An NK/T patient sample positive for nuclear PFKP expression shows expression of CXCR4 and CDK6 on a set of serial sections. Enlargement shows that the expression of CXCR4 and CDK6 were detected in the same region.

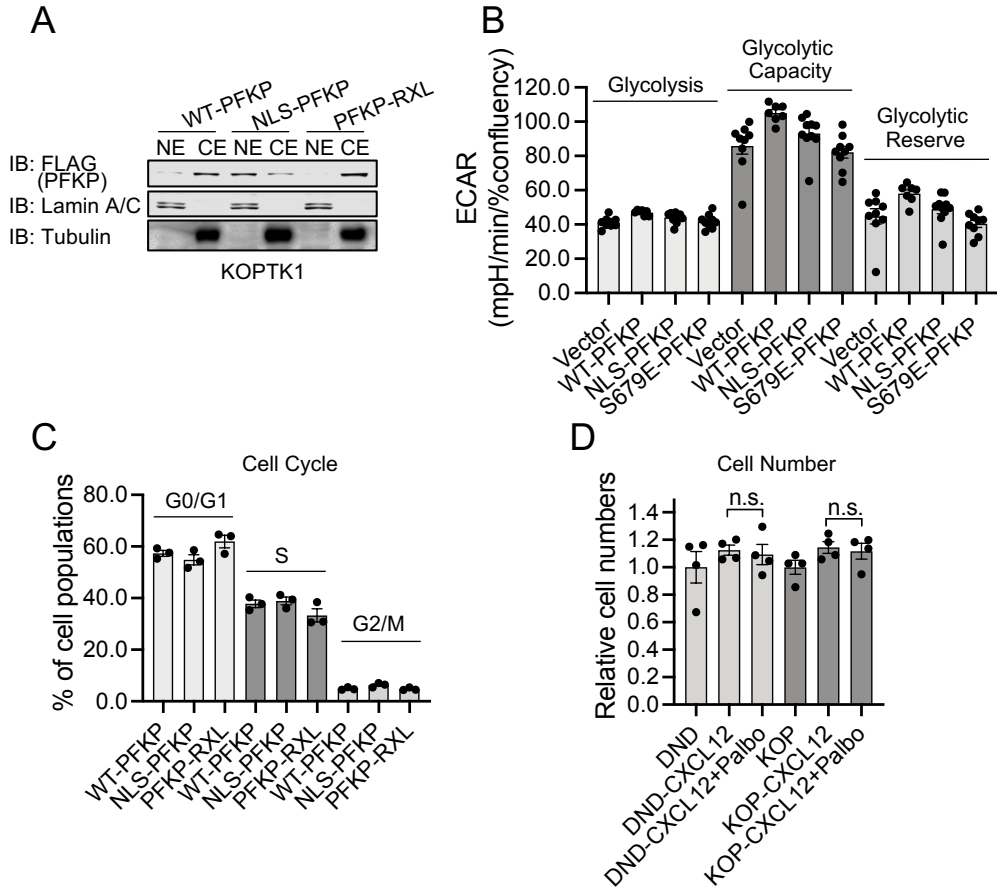
References

1. Wang H, Nicolay BN, Chick JM, Gao X, Geng Y, Ren H, et al. The metabolic function of cyclin D3-CDK6 kinase in cancer cell survival. *Nature*. 2017;546(7658):426-30.
2. Boyd KE, Wells J, Gutman J, Bartley SM, and Farnham PJ. c-Myc target gene specificity is determined by a post-DNA binding mechanism. *Proc Natl Acad Sci U S A*. 1998;95(23):13887-92.
3. Yu J, Cao Q, Mehra R, Laxman B, Yu J, Tomlins SA, et al. Integrative genomics analysis reveals silencing of beta-adrenergic signaling by polycomb in prostate cancer. *Cancer Cell*. 2007;12(5):419-31.
4. Yu J, Yu J, Mani RS, Cao Q, Brenner CJ, Cao X, et al. An integrated network of androgen receptor, polycomb, and TMPRSS2-ERG gene fusions in prostate cancer progression. *Cancer Cell*. 2010;17(5):443-54.
5. Ghandi M, Huang FW, Jane-Valbuena J, Kryukov GV, Lo CC, McDonald ER, 3rd, et al. Next-generation characterization of the Cancer Cell Line Encyclopedia. *Nature*. 2019;569(7757):503-8.
6. Stark C, Breitkreutz BJ, Reguly T, Boucher L, Breitkreutz A, and Tyers M. BioGRID: a general repository for interaction datasets. *Nucleic Acids Res*. 2006;34(Database issue):D535-9.
7. Huang da W, Sherman BT, and Lempicki RA. Systematic and integrative analysis of large gene lists using DAVID bioinformatics resources. *Nat Protoc*. 2009;4(1):44-57.
8. Langmead B, and Salzberg SL. Fast gapped-read alignment with Bowtie 2. *Nat Methods*. 2012;9(4):357-9.
9. Zhang Y, Liu T, Meyer CA, Eeckhoute J, Johnson DS, Bernstein BE, et al. Model-based analysis of ChIP-Seq (MACS). *Genome Biol*. 2008;9(9):R137.
10. Ramirez F, Dundar F, Diehl S, Gruning BA, and Manke T. deepTools: a flexible platform for exploring deep-sequencing data. *Nucleic Acids Res*. 2014;42(Web Server issue):W187-91.

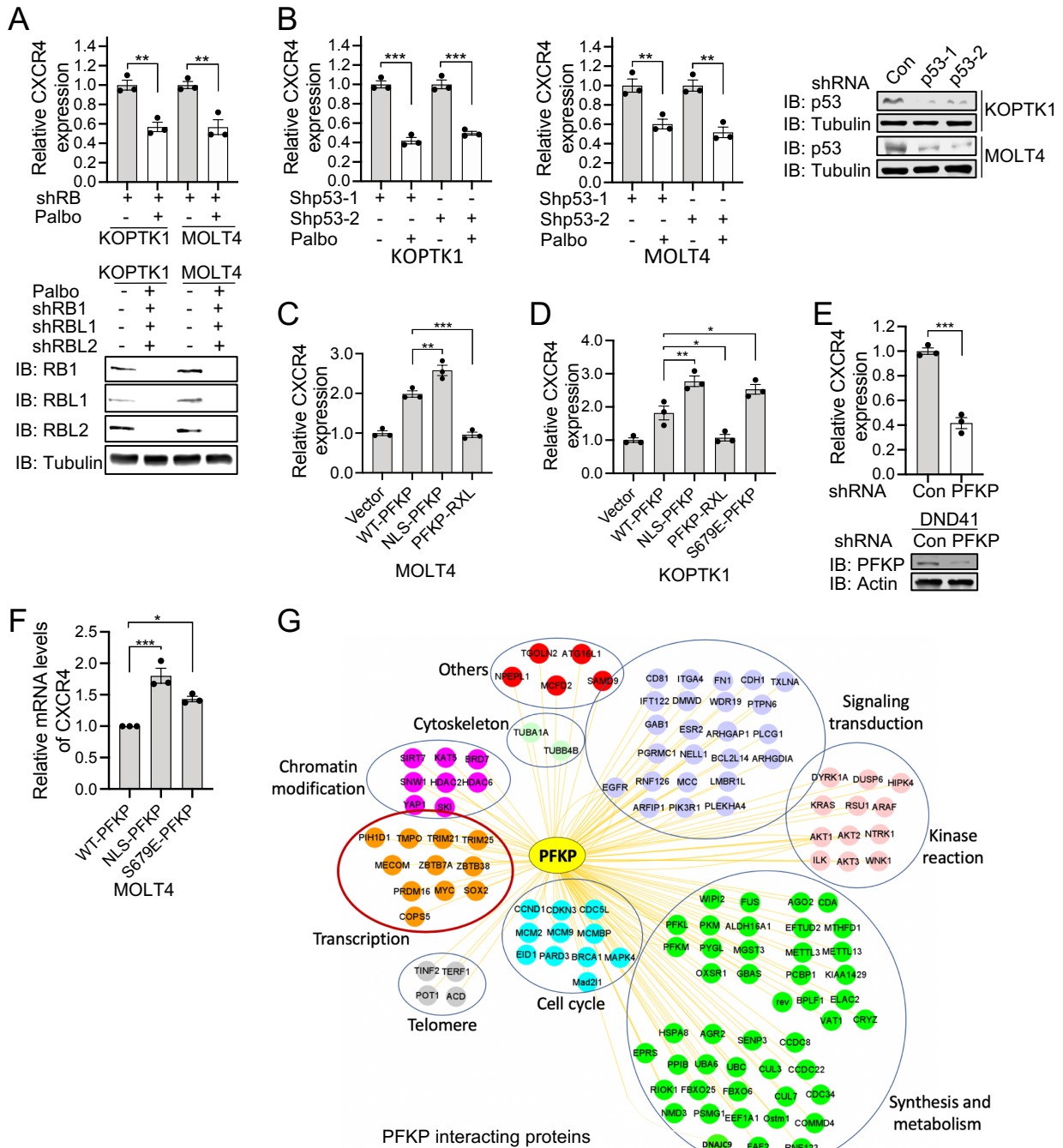


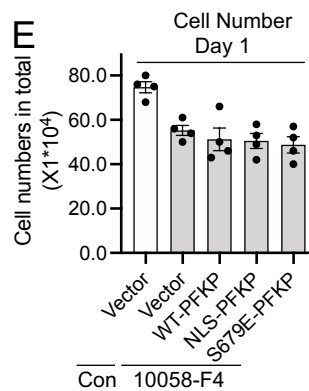
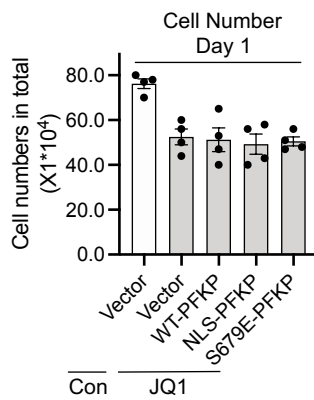
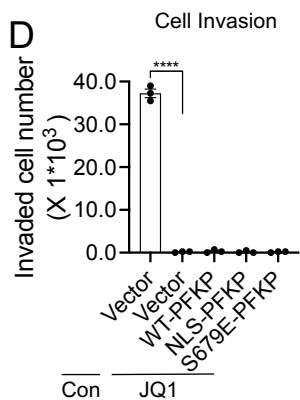
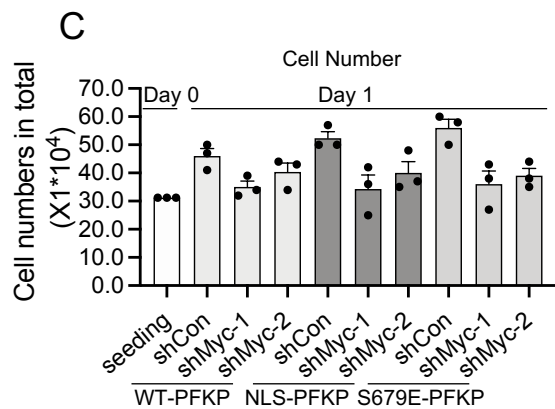
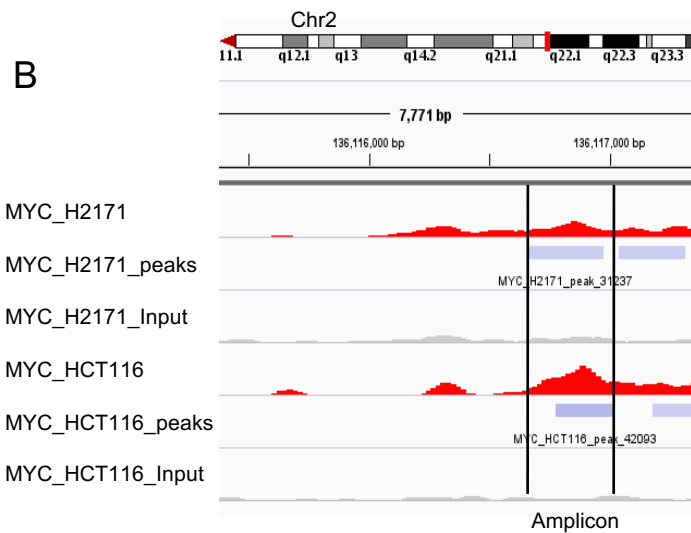
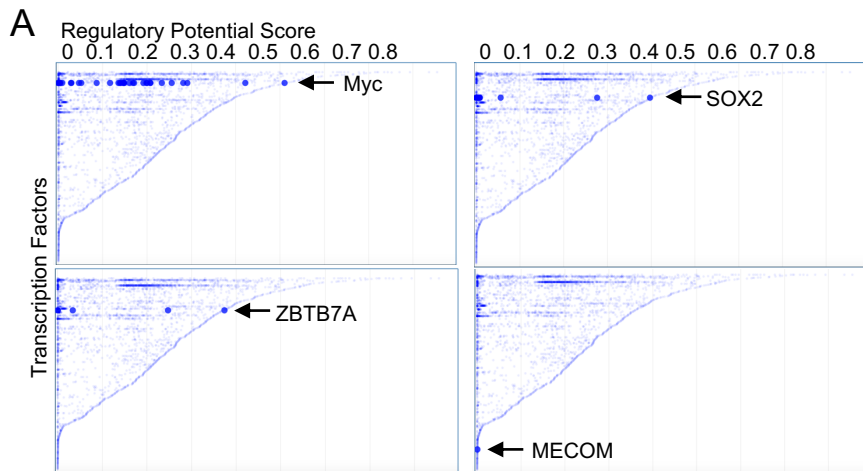
Supplemental Figure 2

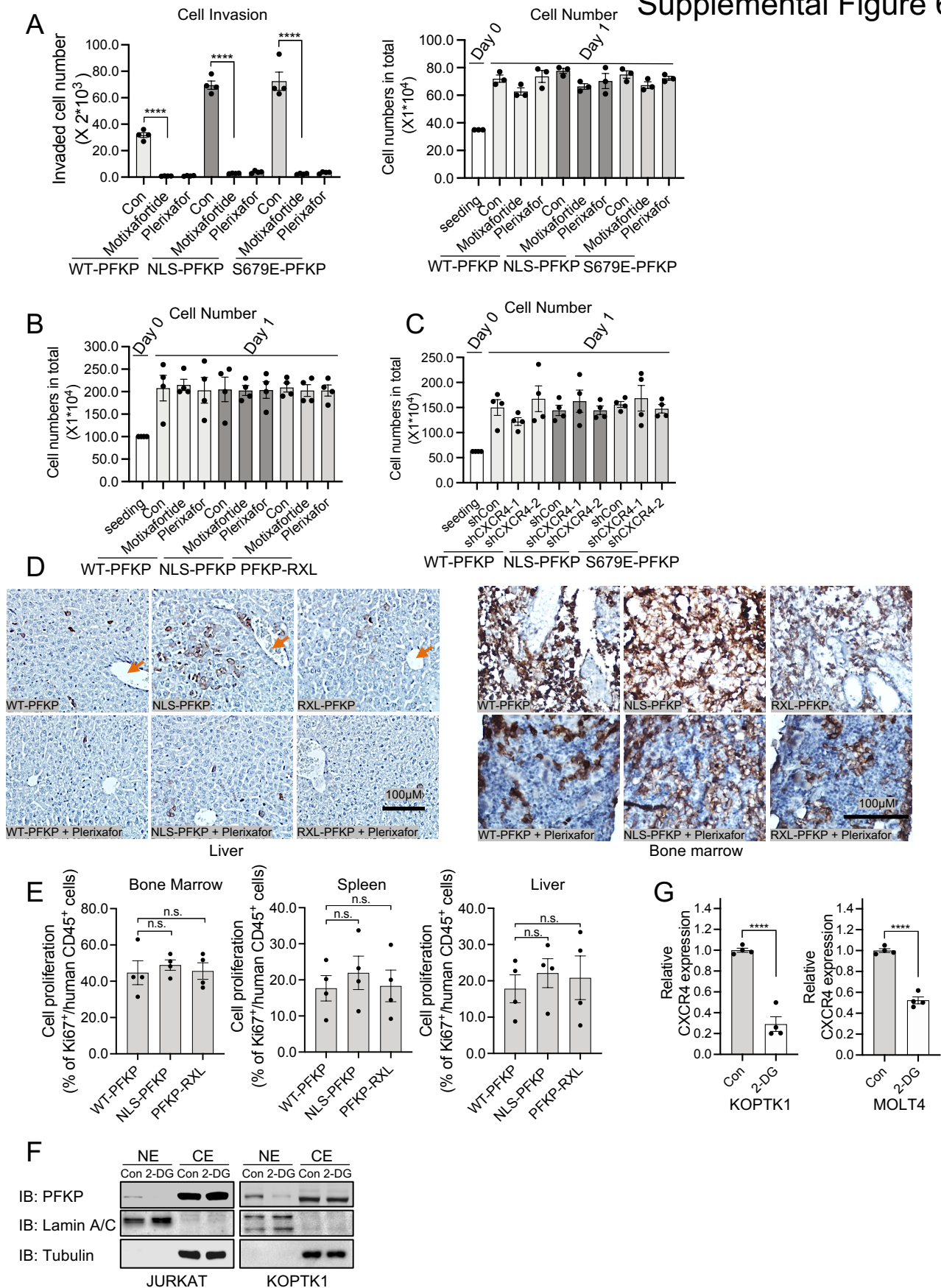




Supplemental Figure 4







Supplemental Figure 7

